Integration of Electrodes with Diphasic Microfluidics for Capacitance Tuning

Charles-Louis Azzopardi, Franck Chollet, Nathalie Tarchichi, Jean-François Manceau
FEMTO-ST Institute, Université Bourgogne Franche-Comté, CNRS UMR 6174
15B Avenue des Montboucons, 25030 Besançon cedex, France
Email: cl.azzopardi@femto-st.fr, franck.chollet@femto-st.fr

***Abstract*—This work reports on the design, the modeling, the simulation, the integration strategy and the preliminary test results of a new variable capacitor using large variation of permittivity obtained by tuning the density of oil-in-water droplet produced with a microfluidic circuit.**

I. Introduction

Tunable capacitors are useful in a wide range of electronics circuit, from oscillators to sensors or matching networks.

A capacitor is used to store electrical charges on two electrodes separated by a gap filled with a dielectric. In this case the capacitance is proportional to :

$$C \propto \epsilon \frac{A}{g} \tag{1}$$

where ϵ is the dielectric permittivity, A the electrodes area, and g the gap between the electrodes. This simple equation gives the parameters that can be modified for tuning the capacitance.

In microelectronics, the tunable capacitor takes usually the form of a reverse biased junction (diode varicap). In this component, biasing the PN junction allows the space charge zone to change width, effectively modifying the 'gap' and the junction capacitance. MEMS allow a more direct change of gap or surface area by using moving electrodes [1]. Finally, although it is not a controlled change, we may note that a change in permittivity is used for measuring humidity with capacitive sensors.

In this work, we propose to explore a new paradigm, where we control dynamically the dielectric material between the electrodes of the capacitor to tune the capacitance in a wide range. In the following sections, we will first describes the principle in more details, simulate it, and finally describe the fabrication procedure for a device that will demonstrate tunable capacitance.

II. Principle

The principle of the variable capacitor shown in Fig. 1 is simple and takes benefit from the big difference existing in the permittivity of water and oil (in our case we have $\epsilon_{r,oil} = 3$ [2] and $\epsilon_{r,water} = 80$). We clearly see that if we fill the gap between the electrodes either with oil or with water we may expect a change in capacitance by a factor proportional to the permittivity ratio (here above 25) a large range compared to varicap or similar component. The trick here is to fill the gap with a controllable density of droplet for continuous control of the average permittivity of the fluid between the permittivity of oil and the permittivity of water.

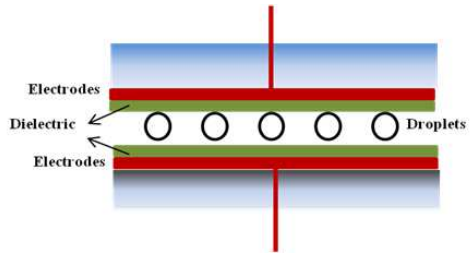

Fig. 1. Principle of operation of the microfluidic tunable capacitor.

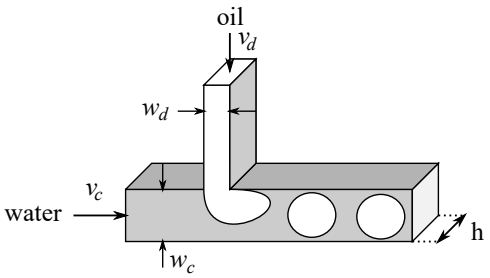

Fig. 2. Generation of monodisperse oil droplet in water at a T-junction.

We have thus proposed to implement a tunable capacitor by incorporating electrodes on silicon/glass chips used for droplet generation. Two versions are explored with electrodes in contact with the fluid or with electrical insulation. In the first case electrolysis limit the use to AC signal or very low voltage, while in the second case the ideal model of the capacitor is changed with additional capacitance coming from the top glass dielectric.

A. Droplet generation

For varying the oil/water ratio between the electrodes, we can show that varying the diameter of droplet in static arrangement (close-packed) does not work, as the ratio between the droplet surface and the total surface is constant (ratio 0.9), independent of the droplet radius, and does not allow effective permittivity change. The control of the device has thus to be dynamic, using change of density of droplet while they are flowing to avoid the apparition of close-packed arrangement.

With droplet generation in T-junction (Fig. 2) in squeezing or dripping regimes, although droplet density variation can

be obtained [3], the diameter, the frequency and the spacing vary in a complex manner and one has to find the appropriate combination of fluids velocity without any possibility for linear control. However we have demonstrated recently [4] the existence of a new droplet generation regime in the T-junction, the balloon-regime, which circumvents this issue. Actually, this generation regime produces droplets of constant diameter independent of phase velocities or width of the continuous phase channel. In fact, the size of the droplet is controlled only by w_d, the dispersed phase channel width, while v_c and v_d controls density or generation rate.

We show in Fig. 3 the effect of varying v_c on the spacing between consecutive droplet. We observe that $l = \frac{v_c}{f} - d$, is linearly varying with the continuous phase velocity for a fixed droplet generation frequency, f.

Control of the generation frequency is achieved with v_d and we have $f = \frac{4w_d}{\pi d^2} v_d$, where d is the droplet diameter, fixed by the width of the dispersed phase channel in the balloon regime [4]. Again the governing equation is linear as a function of the flow rate allowing simple command for controlling the density of droplets.

B. Simulation

An early configuration of the device had the upper electrode (see Fig. 1) positioned atop the sealing glass. This configuration revealed for a single channel of length 3 mm with a width of 100 µm a capacitance in the order of 0.1 pF with a relative change of 20% between water and oil. The small value of the capacitance change compared to what was expected by the simple theory is due in most part to the low capacitance of the glass capacitor. Actually the system can be modeled as two capacitors connected in series :

$$C_s = \frac{1}{\frac{1}{C_g} + \frac{1}{C_f}} = \frac{C_g C_f}{C_g + C_f}$$

where C_g is the capacitance of the glass plate and C_f the fluidic capacitance. As the sealing glass plate is relatively thick (1 mm) compared to the fluidic channel (50 µm), the corresponding capacitance is much smaller than the fluidic capacitance and $C_s \approx C_g$.

For increasing the absolute value of the capacitance and of the variation range we proposed an improved version of the capacitor where we place the electrodes *inside* the fluidic channels with multiple parallel channels and long electrodes. In this case, there are different capacitor configurations possible and for example we may place the electrodes at the top and bottom of the channel as shown in Fig. 1, or, in a configuration simpler to interface, we may use coplanar electrodes placed on one side of the channel.
In the latter case, the electrical field sees the fluid and the underlying glass substrate, resulting in a configuration where we have two capacitors in parallel :

$$C_p = C_g + C_f$$

only C_f is varying with the fluid, roughly as the ration of the respective permittivity of the two fluids, that is

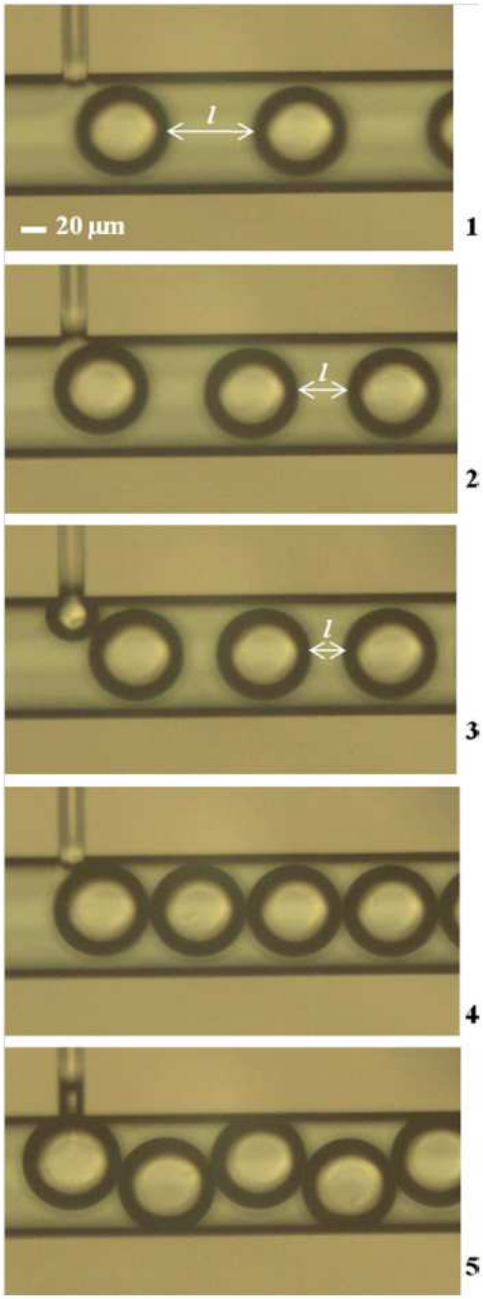

Fig. 3. Variation of spacing between consecutive droplet in the ballon regime as a function of vc with wc = 100 m, wd = 20m, h = 46m, vd = 0,21 cm/s and vc = 0,12 cm/s (1), vc = 0,1 cm/s (2), vc = 0,085 cm/s (3),vc = 0,065 cm/s (4) and vc = 0,062 cm/s (5).

$\epsilon_{r,water}/\epsilon_{r,oil} \approx 26$. Thus, when water is present we have $C_f \gg C_g$ and $C_{water} \approx C_f$. When the oil is present, we note that the permittivity of oil is roughly equal to the glass substrate permittivity, that is $C_{oil} \approx 2C_g$. Thus the expected relative variation of capacitance in the coplanar configuration is given by :

$$\Delta C_p = \frac{C_{water} - C_{oil}}{C_{oil}} \approx \frac{C_{water}}{C_{oil}} \approx \frac{C_f}{2C_g} \approx \frac{\epsilon_{r,water}}{2\epsilon_{r,oil}} \approx 13$$

We verified this simple model by simulating the capacitance

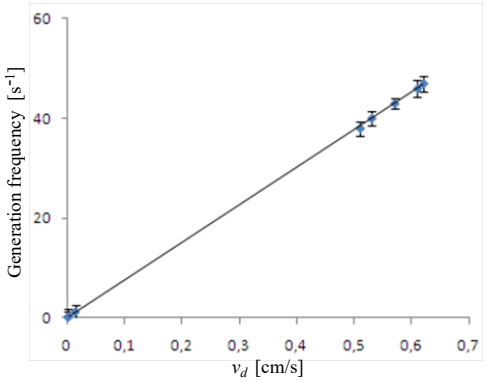

Fig. 4. Variation of droplet generation frequency (droplet/s) as a function of the dispersed phase velocity v_d (cm/s).

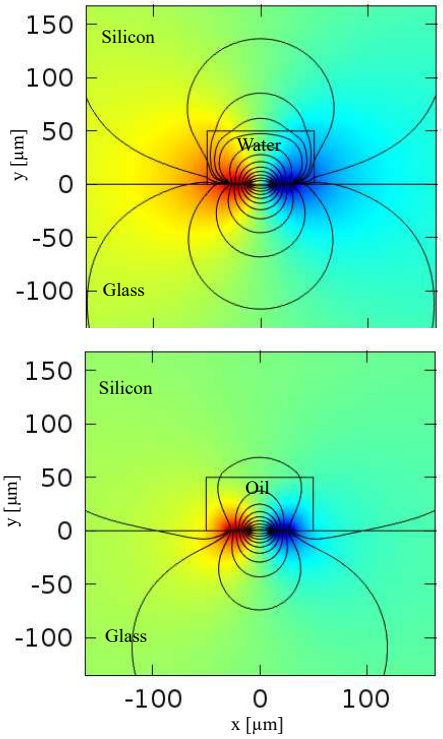

Fig. 5. Numerical simulation of the electrostatic field in the structure for a channel filled with water (top) and oil (bottom).

of this structure using COMSOL Multiphysics. For a pair of electrodes 20 µm wide separated by 20 µm, placed on a glass substrate and with a channel of silicon with a cross-section of 100 µm × 50 µm, we find for water a capacitance of 568 pF/m and for oil [2], the capacitance drops to 57 pF/m. That is a variation by a factor of 10 close to the estimate obtained with the approximate model.

III. Fabrication

According to the simulation, we propose a new device layout as shown in Fig. 6 where we have a droplet generator connected to a long meander channel where the electrodes are located.

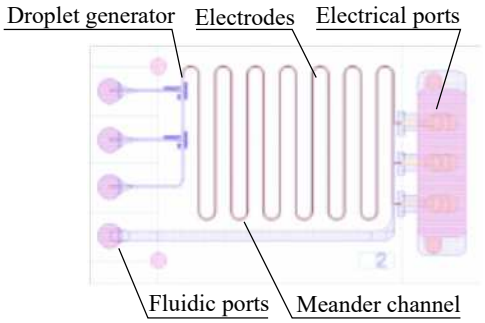

Fig. 6. Layout of a chip with microfluidic (left) and electric (right) interfaces for variable capacitor.

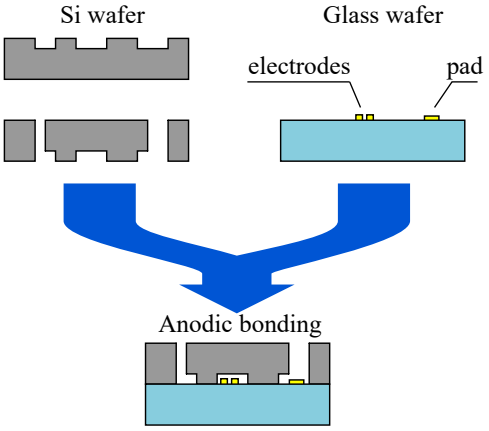

Fig. 7. General process flow.

The process flow is based on the assembly of a silicon wafer patterned with microfluidic channels and fluidic ports and a glass wafer carrying the capacitor electrodes as shown in Fig. 7.

We first pattern the microfluidic channels in the frontside of a silicon wafer. The silicon wafer is first bathed in fresh piranha (H_2O_2 24 ml/H_2SO_4 40 ml) for 5 min to remove any contaminant and obtain repeatable surface energy. The wafer is then baked at 150°C for 10 min to remove adsorbed water on the surface and left 2 min to cool back to cleanroom temperature. After adhesion promoter deposition (TiPrime baked at 120°C for 4 min) we spin-coat AZ9620 at 4000 rpm, bake it 5 min at 105°C and wait for 5 min for hydration. The wafer is then exposed in an EVG620 double side mask aligner with a dose of about 550 mJ. After development (AZ 400K 25 ml : DI water 100 ml) and thorough rinsing and drying, the wafer is etched in an SPTS Pegasus-Rapier DRIE system to a depth of 50 µm. After resist stripping and piranha cleaning, the wafer is ready for the patterning of the fluidic ports in the backside of the silicon wafer.

We protect the wafer front side with a thin layer of S1813 photoresist before we coat it on the backside with a thick layer of AZ9620 at 2000 rpm (about 9 µm thick) and bake it for 6 min at 105°C. After 5 min hydration, the wafer is exposed with a dose of 750 mJ and the pattern developed as

previously. Etching through the wafer, in our case to provide the fluidic access holes, remains a relatively cumbersome procedure as it needs to avoid leakage of the helium used to cool the backside of the wafer when the through holes open. We divided the etching in two steps. First we used an Alcatel A501 DRIE system with mechanical clamping to etch about 400 µm of the 500 µm thick wafer, and in a second step we mount the wafer on an oxidized support wafer with a thin layer of Crystal Bond spread on a hotplate at 120°C for etching in the SPTS Pegasus-Rapier chamber with electrostatic clamping. This method solves different issues: the electrostatic clamp forbids using patterned bottom of wafer and protective photoresist, but using mechanical clamp on a stack of two wafers often causes breakage as the intermediate layer (here Crystal Bond) is rarely uniformly coated. After etching, the stacked wafers are left in acetone for several hours, separating the etched silicon wafer from the support wafer.

The glass wafer electrodes are patterned using lift-off (with LOR and S1813 photoresist) of a Cr 20 nm/Ni 200 nm/Au 150 nm stack. The nickel intermediate layer has two functions : it acts as a diffusion barrier to prevent diffusion of gold during the later anodic bonding and also it makes a stronger mechanical layer for preventing damage when spring loaded contact will touch the pad surface.

For preparing the two surfaces before anodic bonding, we use fresh piranha on the silicon substrate and sulfochromic acid at room temperature on the metalized glass plate, to avoid damaging the metal layer. Prior to bonding, the glass wafer and the silicon wafers are aligned in the EVG 620 double side mask aligner with an accuracy <5µm. The anodic bonding is performed in an EVG 501 bonder at a reduced temperature (about 300°C) to decrease the deleterious effect of temperature on the metal layer.

Finally, the chips are diced with a Disco DAD 321 saw after being mounted glass on top on an adhesive tape. The tape protects from contamination the openings in the silicon wafer during dicing. The last operation is to plug the metal line access hole. Actually, the metal could prevent anodic bonding and the line exits the microfluidic channel through an access channel in silicon placed close to the electric port. We may use different type of liquid adhesive to perform this task, before the fluidic and electrical tests can be performed.

We have also fully developed a test bench that solves the problem of simultaneous electrical and fluidic connections as shown in Fig. 8, where spring contacts in one side of the chip are used for electrical connection whereas a rigid connector with O-ring is used on the other side for the fluids input and output.

IV. Conclusion

We propose a variable capacitor based on microfluidic where we continuously change the average permittivity of the fluid between the two capacitor electrodes by taking benefit of the large difference of permittivity between oil and water. The device proposes to modify dynamically the ratio between oil and water using a generator of oil droplets in water with a T-junction in balloon regime. We have presented evidence suggesting that this regime should give a simple linear tuning of the capacitance. Simulation shows that a variation of capacitance by a factor of 10 can be reached, and other operation mode may also be used (using the silicon substrate as an electrode) that could further improve this figure. Final tests and characterization of the component will be reported during the conference.

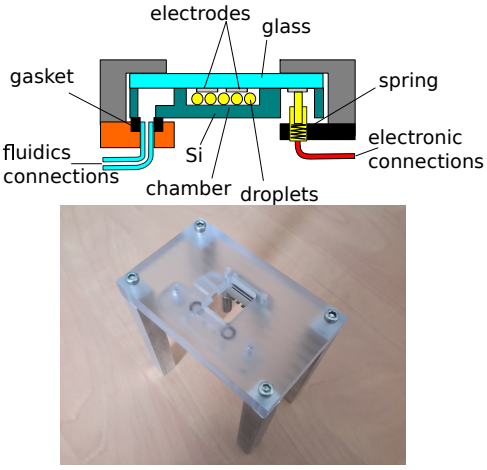

Fig. 8. Prototype of microfluidic/electric interface for variable capacitor.

Acknowledgment

This work was supported by the french RENATECH network and its FEMTO-ST technological facility. The authors would like to thank the Labex ACTION program (Contact No. ANR-11-LABX-0001-01) for the financial support.

References

[1] W. Tang, T. Nguyen, and R. Howe, "Laterally driven polysilicon resonant microstructures," *Sens. and Actuat.*, vol. 20, pp. 25–32, 1989.

[2] Z. H. Shah and Q. A. Tahir, "Dielectric properties of vegetable oils," *Journal of Scientific Research*, vol. 3, no. 3, pp. 481–492, 2011.

[3] N. Tarchichi, F. Chollet, and J.-F. Manceau, "Oil-in-water droplets generation in dripping regime with channel partial wetting," *Micro and Nanosystems*, vol. 6, no. 3, pp. 145–155, 2014.

[4] ——, "New regime of droplet generation in a T-shape microfluidic junction," *Microfluidics and Nanofluidics*, vol. 14, pp. 45–51, 2013.